

Emergence of the Primacy Effect in Structured State-Space Models

Takashi Morita

Academy of Emerging Sciences, Chubu University

tmorita@alum.mit.edu

Abstract

Human and animal memory for sequentially presented items is well-documented to be more accurate for those at the beginning and end of the sequence, phenomena known as the *primacy* and *recency* effects, respectively. By contrast, artificial neural network (ANN) models are typically designed with a memory that decays monotonically over time. Accordingly, ANNs are expected to show the *recency* effect but not the *primacy* effect. Contrary to this theoretical expectation, however, the present study reveals a counterintuitive finding: a recently developed ANN architecture, called *structured state-space models*, exhibits the primacy effect when trained and evaluated on a synthetic task that mirrors psychological memory experiments. Given that this model was originally designed for recovering neuronal activity patterns observed in biological brains, this result provides a novel perspective on the psychological primacy effect while also posing a non-trivial puzzle for the current theories in machine learning.

1 Introduction

Human and animal memory for sequentially presented items is well-documented to be more accurate for those appearing at the beginning and end of the sequence—phenomena known as the *primacy* and *recency* effects, respectively (Ebbinghaus, 1913; Murdock, 1962; Glanzer and Cunitz, 1966). For example, when a sequence of random integers such as 49, 75, ..., 5, 38 is presented in that order, the initial (49, 75) and final (5, 38) items are more likely to be recalled accurately at the end of the presentation.

By contrast, artificial neural network (ANN) models are typically designed with a memory that decays monotonically over time (Bengio et al., 1994; Jaeger, 2001; Jaeger and Haas, 2004). Thus, ANNs are expected to show the *recency* effect but not the *primacy* effect.

Contrary to this theoretical expectation, however, the present study reveals a counterintuitive finding: a recently developed ANN architecture—called *structured state-space models* (Gu et al., 2020, 2022b)—exhibits the primacy effect when trained and evaluated on a synthetic task that mirrors psychological memory experiments. Given that this model was originally designed for recovering neuronal activity patterns observed in biological brains, this result provides a novel perspective on the psychological primacy effect while also posing a non-trivial puzzle for the current theories in machine learning.

The remainder of this paper is organized as follows. The next section first reviews ANN models for time-series processing. After this preliminary discussion, the Methods section details the task and model specifications of the present study, and the subsequent section presents the results. Finally, the Discussions section summarizes the findings and discusses their implications in relation to previous research.

2 Preliminaries on ANNs for Time-Series Processing

2.1 Recurrent Neural Networks

The traditional ANN-based approach to time-series processing relies on recurrent neural networks (RNNs; Elman, 1990). RNNs sequentially process inputs, updating their internal state (represented by a real-valued vector) at each time step based on both the current input and the previous state. The output is then generated through a feedforward

transformation of this internal state at each step. In other words, RNNs map input time series to target output sequences through the latent dynamics of their internal state.

Theoretically, RNNs possess Turing-complete computational power, meaning they can simulate an arbitrary computational model in an “idealized” setting (Siegelmann and Sontag, 1992, 1995; Siegelmann, 1999). This theoretical capability has driven widespread applications of RNNs in domains such as language modeling (Sundermeyer et al., 2012; Graves, 2013), speech synthesis (Kalchbrenner et al., 2018), and weather nowcasting (Shi et al., 2015).

However, the “idealized” computational properties of RNNs are unattainable in empirical implementations. For instance, when deployed on standard computers, the weight parameters of RNNs can only be represented with finite precision (Chen et al., 2018; Weiss et al., 2018), preventing them from storing an unbounded number of observations. Additionally, RNNs exhibit memory decay over time, which has led researchers to explore methods for extending their memory retention capabilities (Hochreiter and Schmidhuber, 1997; Arjovsky et al., 2016; Neil et al., 2016; Chang et al., 2017; Jing et al., 2017, 2019).

2.2 Structured State-Space Models

Recently, researchers have found that continuous-time models can achieve more persistent memory retention than discrete-time RNNs (Zhang et al., 2018; Voelker et al., 2019; Gu et al., 2020). The fundamental principle underlying these models is the polynomial approximation of observed signals (called the *HiPPO* framework; Gu et al., 2020). Specifically, given a *single*-channel input signal $x(\cdot)$, represented as a function of time, its approximation up to a given time point t can be approximated by a linear combination of polynomials:

$$x|_{\leq t}(\cdot) \approx \sum_{n=0}^{N-1} h_n(t) P_n(\cdot)$$

where P_n denotes the basis polynomial of degree n and $h_n(t)$ are the optimal coefficients for the approximation at time t .¹ Then, these coefficients offer a finite- and constant-dimensional representation of the input signal up to time t . The framework can be naturally extended to multi-channel signals by performing channel-wise approximations in parallel, yielding $h_n^{(m)}(t)$ for each channel m .

For the polynomial coefficients to serve as a “memory” of the input signal, their temporal evolution must be trackable in an *online* manner; that is, the polynomial approximation at time t should not refer back to past values of the input signal, $x|_{\leq t}(s)$ ($0 \leq s < t$). Fortunately, for certain families of polynomials, including Legendre, Laguerre, and Fourier basis,² the coefficient dynamics can be described by an ordinary differential equation (ODE; Gu et al., 2020):

$$\frac{d}{dt} \mathbf{h}(t) = A\mathbf{h}(t) + Bx(t) \quad (1)$$

where $\mathbf{h}(t) := (h_0(t), \dots, h_{N-1}(t))^T$, and A and B are matrices of size $N \times N$ and $N \times 1$, respectively. The values on A and B —referred to as the *state* and *input* matrices, respectively—depend on the choice of the underlying polynomial basis, and can also be adjusted via gradient-based optimization. A feedforward transformation of the state vector $\mathbf{h}(t)$ (achieved via left-multiplication by another matrix C) yields a (possibly multi-channel) output signal $\mathbf{y}(t) = C\mathbf{h}(t) \in \mathbb{R}^M$.³ The resulting mapping $x \mapsto \mathbf{y}$ is termed the *structured state-space model* (hereinafter abbreviated as *SSM*; Gu et al., 2021, 2022b).

In practice, continuous-time recordings of an input signal $x(t)$ are not available; instead, empirical data consist of discrete-time samples at $t = t_1, \dots, t_L$. Consequently, the SSM matrices must also be discretized in order to convert the ODE in Eq. 1 to a discrete recurrent system, analogous to RNNs:

$$\mathbf{h}(t_j) = \bar{A}\mathbf{h}(t_{j-1}) + \bar{B}x(t_j) \quad (2)$$

¹The optimal coefficients can be determined as $h_n(t) = \langle x|_{\leq t}, P_n \rangle = \int x|_{\leq t}(s) P_n(s) d\mu^{(t)}(s)$ when $\{P_n\}_{n=0}^{N-1}$ form an orthogonal basis with respect to the time-dependent measure $d\mu^{(t)}(\cdot)$.

²The Fourier approximation (or transform) is not based on polynomials, but the theory can be generalized to incorporate it by taking the complex-valued basis $z^n := e^{2\pi i n s}$ and a measure on the unit circle (Gu et al., 2020).

³The general formulation of the SSM incorporates an additional matrix D , which establishes a direct feedforward connection between the input and output signals, expressed as $\mathbf{y}(t) = C\mathbf{h}(t) + D\mathbf{x}(t)$. In practice, however, D is often set to the identity matrix, effectively reducing the feedforward transformation to a simple residual connection (He et al., 2016).

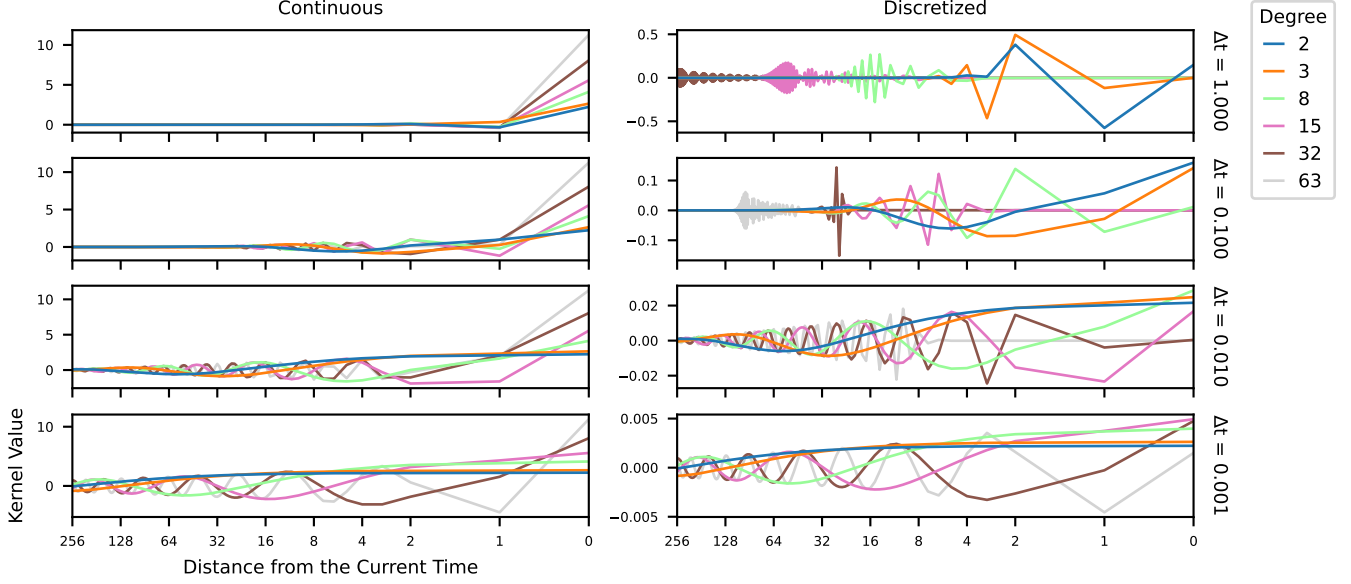


Figure 1: Illustration of the continuous (left; $K(\tau) := e^{\tau A} B$) and discretized (right; $\bar{K}_j := \bar{A}^j \bar{B}$) SSM kernels based on Legendre polynomials with an exponentially decaying measure (Gu et al., 2023). To aid intuitive understanding (particularly for readers unfamiliar with convolutional operations), the horizontal axis has been flipped, so that kernel values multiplied with past inputs appear on the left (unlike in the standard visualization of convolutional kernels, where they are placed on the right). The distinct line colors represent selected entries of the kernel vectors, $K_N(\tau)$ and $\bar{K}_{j,n}$, each corresponding the approximating polynomial of degree $n \in \{2, 3, 8, 15, 32, 63\}$. The kernels were evaluated at $\tau = j\Delta t$ for $j = 0, \dots, 255$ and $\Delta t \in \{0.001, 0.01, 0.1, 1.0\}$. Increasing Δt results in growing discrepancies between the continuous and discretized kernels.

where \bar{A} and \bar{B} represent the discretized versions of A and B , respectively. A commonly used discretization technique is the bilinear method (Tustin, 1947), which yields:

$$\bar{A} := \left(I - \frac{\Delta t}{2} A \right)^{-1} \left(I + \frac{\Delta t}{2} A \right) \quad \bar{B} := \left(I - \frac{\Delta t}{2} A \right)^{-1} \Delta t B$$

where $\Delta t := t_{j+1} - t_j$ ($\forall j = 1, \dots, L-1$) defines the time-step size. This time-step parameter is treated as learnable, allowing the model to automatically adjust the time scale of its state-space dynamics to align with that of the input signal. Moreover, in multi-channel settings, the model can represent multi-scale dynamics by assigning distinct $\Delta t^{(m)}$ values to each channel m .

This flexibility extends the applicability of SSMs to inherently discrete data lacking overt continuous dynamics (e.g., text languages; Gu and Dao, 2024; Dao and Gu, 2024); the model can jointly learn latent representations (or embeddings) of discrete inputs along with their (pseudo-)continuous dynamics via gradient-based optimization. Furthermore, SSMs can be hierarchically stacked to construct deeper and more expressive ANNs, where each layer processes latent signals received from lower layers.

Previous studies have identified that the time-step size, Δt , as a critical factor in determining the success/failure of SSMs. Intuitively, a small Δt results in minor state updates, yielding slow dynamics in the state space, $\mathbf{h}(t_{j+1}) - \mathbf{h}(t_j)$; conversely, a large Δt induces rapid state transitions (Gu et al., 2021; Gu and Dao, 2024). As a consequence, Δt governs the memory decay properties of the SSM; although the models assume an exponentially decaying measure in continuous time (particularly when employing Legendre/Laguerre polynomials; Gu et al., 2023), choosing small Δt values can allocate relatively large weights to input samples from distant time steps, thereby compromising single-step discriminability, which is better preserved with larger Δt (see left panels in Fig. 1).

It is also important to note that discretization methods are generally designed under the assumption of sufficiently small Δt , for effectively approximating the limit $\Delta t \rightarrow 0$. Consequently, setting Δt too large introduces discrepancies between the continuous and discretized dynamics (as illustrated by the contrast between the left vs. right panels in Fig. 1).

2.3 Finite-Queue/Markov Models

Finally, it is worth mentioning finite-queue/Markov models, which encompass the current goldstandard architecture of ANNs, Transformer (Vaswani et al., 2017). These models are equipped with an explicit storage mechanism that retains raw observation records up to a prespecified limit. Formally, they enable arbitrary computations at a given discrete time j while maintaining full access to the most recent M observations, x_{j-M+1}, \dots, x_j . At each time step, the oldest observation (x_{j-M}) is discarded as new data enter the storage buffer.

By design, finite-queue/Markov models do not exhibit the primacy effect once earlier observations inputs fall outside the accessible memory window. Instead, they align with the classical view of biological short-term memory Miller (1956), which has traditionally been linked with the recency effect (Waugh and Norman, 1965; Glanzer and Cunitz, 1966; Atkinson and Shiffrin, 1968).

Nonetheless, given sufficient computational resources, the memory capacity of modern models like Transformers can cover most empirical sequences, rendering the out-of-window effects negligible in practice. In such cases, models with naive implementations assign equal importance to all observations. Most notably, the canonical Transformer is inherently agnostic to input order in the absence of positional encoding (Vaswani et al., 2017), implying a form of bias-free memorization. Nevertheless, as discussed in the following section, even such unbiased models can exhibit the primacy effect when trained on specific datasets or tasks.

2.4 Data-Driven Primacy Effect in Language Models

Several prior studies have documented the primacy effect of ANNs trained on the autoregressive language modeling task. Wang et al. (2023) investigated positional biases in a Transformer-based large language model (LLM) using a prompting-based approach. Specifically, a list of action or event labels was sequentially presented (e.g., “Label 1: change_pin”, “Label 2: card_arrival”, “Label 3: activate_my_card”). The model was then given a query prompt specifying a target action/event (e.g., “Target Text: I need a new PIN.”) along with an instruction statement (e.g., “Which label matches the intent expressed in the Target Text?”). The primacy effect was observed as a greater frequency of the initially presented labels in the model’s responses.⁴ Comparable findings have been reported across different LLM implementations and benchmark datasets (Eicher and Irgolić, 2024; Guo and Vosoughi, 2024; Janik, 2024; Liu et al., 2024).

Xiao et al. (2024) found that Transformer-based LLMs allocated disproportionate attention to initial tokens, regardless of their informational salience in the text (a phenomenon they termed *attention sinks*). Furthermore, retaining these initial tokens even after they fall outside the predefined input window was found to enhance model performance.

Since the Transformer architecture is inherently position-agnostic—lacking an intrinsic ordering mechanism apart from external positional encodings (Vaswani et al., 2017)—the primacy effects observed in these studies must stem from the statistical properties of the training data or task design. Wang et al. argued that LLMs inherit cognitive biases from human-generated linguistic data. Xiao et al. suggested that the nature of the language modeling task itself encourages prioritization of initial tokens, as they are repeatedly used as inputs for autoregressive predictions, reinforcing attention allocation to them.

In contrast to prior investigations, the present study examines the emergence of the primacy effect in ANNs preventing the inheritance of human-induced bias. Specifically, the models are trained on a synthetic memorization task designed based on psychological experiments conducted with humans and other animals (Thompson and Herman, 1977; Sands and Wright, 1980; Wright et al., 1985). The following section details the task formulation and the model architecture.

⁴According to the published code, the indices assigned to the labels (e.g., “2” in “Label 2: card_arrival”) consistently corresponded to their order of presentation; that is, “Label j : xxx” was never listed before “Label j' : yyy” if $j' < j$, even though the label contents (“xxx” and “yyy”) were disassociated from the label indices and ordered randomly. Hence, the reported primacy effect could be attributed to a bias in model *responses* toward lower-indexed labels, which appear more frequently than larger integers (e.g., 2 vs. 67), rather than to greater attentions to initially presented labels.

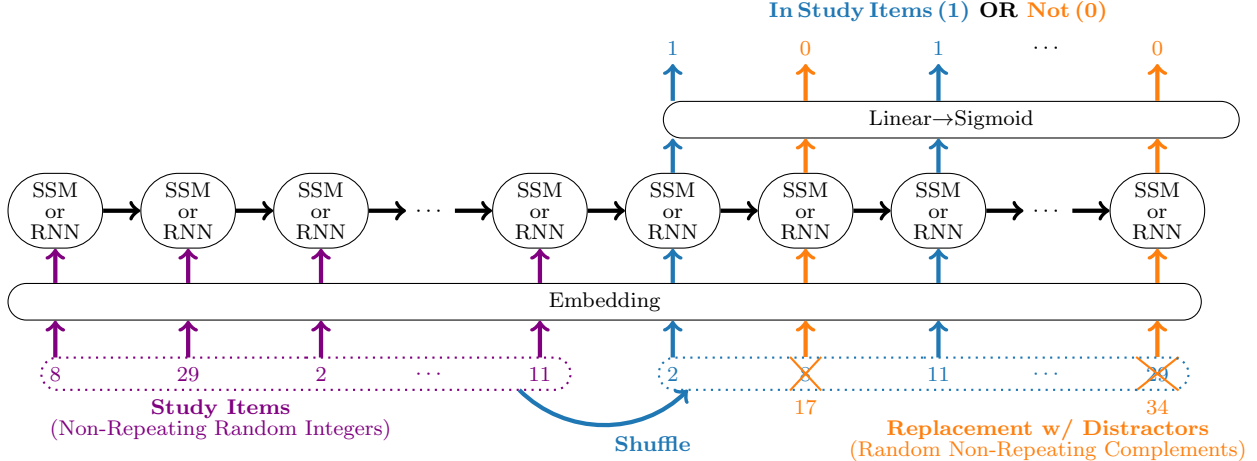


Figure 2: Schematic illustration of the binary memory verification task.

3 Methods

3.1 Task

The memorization patterns of ANNs were assessed using the binary memory verification task (Fig. 2; a.k.a. *serial probe recognition*; Wickelgren and Norman, 1966; Thompson and Herman, 1977; Sands and Wright, 1980; Wright et al., 1985).⁵ In this task, the models were first presented with a sequence of randomly generated, non-repeating integers (hereinafter referred to as *study items*). Subsequently, they received another sequence of integer queries and were trained to determine whether each query token was present (labeled as 1) or absent (labeled as 0) in the study items. To construct these queries, the study items were first shuffled, and then, with a probability of $p = 0.5$, each shuffled token was replaced with a randomly sampled integer from the complement set of the study items (termed *distractors*).

The task hyperparameters were manually adjusted to prevent the models from achieving perfect accuracy. Specifically, the input length was set to $L \in \{64, 128, 256\}$, and the vocabulary size was fixed at $K := 4096$. Each model underwent ten independent training runs with different random seeds. For evaluation, 1024 sets of integers were held out as test data, ensuring that these integer combinations never appeared as study items in the training set, regardless of their order.

To build test sequences, the held-out study items were randomly ordered, and queries were generated by first shuffling and then cyclically shifting them (e.g., $(2, 8, 11, 29) \mapsto \{(2, 8, 11, 29), (8, 11, 29, 2), (11, 29, 2, 8), (29, 2, 8, 11)\}$). This design ensured that each study item was queried in all L possible positions. Finally, either the even- or odd-indexed query positions were replaced with random distractors, resulting in a total of $1024 \times L \times 2$ test sequences per trial.

3.2 Models

The models used for the binary memory verification task comprised three layers, as illustrated in Fig. 2. In the first layer, the input integers were embedded into 256-dimensional real-valued vectors. These embeddings were shared between study items and query tokens. The resulting sequence of vectors was then processed by the SSM/RNN, whose outputs were linearly projected onto binary logits to determine whether each query token was present in the study items.

⁵The most widely adopted task for assessing the primacy effect in human memory is *free recall*, in which participants are presented with a sequence of items and subsequently asked to recall them in an order-agnostic manner (Murdock, 1962; Glanzer and Cunitz, 1966). While this paradigm can be technically formulated as a loss function for ANNs (Cuturi, 2013), initial explorations of this study revealed that model performance remained suboptimal under this approach, yielding lower accuracy than in theoretically more demanding tasks requiring order-sensitive reconstruction. Consequently, the present study adopted the more machine learning-friendly task based on binary verification. Remarkably, this task has also been used to assess the memory capacity of non-human animals, which are unable to perform free recall (Thompson and Herman, 1977; Sands and Wright, 1980; Wright et al., 1985).

This study primarily examined the single-layer S4 model as the goldstandard implementation of the SSM (Gu et al., 2022b).⁶ The model encoded the channel-wise dynamics of the input embeddings in a complex-valued space, with its outputs subsequently projected back into the real domain by discarding imaginary components. The state and input matrices (A and B in Eq. 1) were initialized to approximate each channel’s trajectory using Legendre/Laguerre polynomials of degrees 0–63 (HiPPO-LegS/LagT) or a Fourier basis $\{s_0, c_0, \dots, s_{31}, c_{31}\}$, where $s_n(t) := \sqrt{2} \sin(2\pi nt)$ and $c_n(t) := \sqrt{2} \cos(2\pi nt)$ (HiPPO-Fout, Fourier Recurrent Unit; Zhang et al., 2018; Gu et al., 2020, 2023). The matrices were discretized by the bilinear method (Tustin, 1947).

For comparison, a single-layer long short-term memory (LSTM) network was also evaluated (Hochreiter and Schmidhuber, 1997). LSTM has been the goldstandard RNN architecture for various time-series processing tasks, including language modeling (Sundermeyer et al., 2012; Graves, 2013). The dimensionality of both hidden and cell states was set to 256.

Another well-established baseline worth considering is the Transformer architecture (Vaswani et al., 2017), equipped with a sufficiently long memory window. However, it turned out that the Transformer can easily achieve perfect accuracy on the adopted task—even at the maximal levels of input length and vocabulary size implementable within the available computational resources—thereby failing to incur the memory load necessary for evaluating the primacy effect.⁷ Consequently, the Transformer is excluded from the main results reported in the next section; instead, the Appendix provides a detailed explanation of how it can solve the memory verification task, with particular emphasis on the role of its attention mechanism.

The models were trained for 300,000 iterations using the Adam optimizer with parameters $(\beta_0, \beta_1) := (0.9, 0.99)$ (Kingma and Ba, 2015). Batch size was set to 512. The learning rate was linearly increased from 0.0 to 0.001 over the first 1,000 iterations (*warmups*) and subsequently decayed according to the cosine annealing schedule Loshchilov and Hutter (2017). To prevent gradient explosion, the gradient norm was clipped at 1.0. The Python code for the experiments is available at <https://github.com/An0nym0usAuth0r/NeuralPrimacyEffect.git>.

4 Results

4.1 Emergence of the Primacy Effect

Fig. 3 reports the accuracy of the binary memory verification task across all combinations of memorization and verification times. The brightness of each cell in the square heatmaps indicates the accuracy for study items that were presented at the time indexed by the corresponding row and queried at the time indexed by the corresponding column. That is, they report the proportion of true positives against false negatives (i.e., the *recall* score). Additionally, the top separate row of each panel displays the accuracy for distractor queries (integers not included among the study items), capturing the prevalence of true negatives over false positives. Just below it, the second row summarizes the average accuracy across memorization times (rows). Similarly, the rightmost separate column represents the average accuracy across all verification times (columns).

The binary memory verification performance of the SSM model was highest for study items presented at the beginning of the sequence, demonstrating a clear primacy effect (Fig. 3A–G). The model maintained high accuracy across different query timings (as indicated by the bright colors in the top rows of the heatmaps), provided that the sequence length did not exceed its capacity (see the accuracy decline in Fig. 3G, where $L = 256$). In other words, memory for the initial study items exhibited minimal decay over time.

By contrast, the LSTM did not display this primacy effect; its accuracy was uniform across both the memorization and verification phases (Fig. 3H).

Interestingly, the SSM’s accuracy for the most recently presented study items was lowest when they were queried immediately after their initial presentation in the memorization phase (indicated by the dark colors in the bottom-left region of the heatmaps). This suggests a temporal delay between the encoding of study items and their effective retrieval.

⁶Recent studies have shown that the state matrix (A) of S4 can be simplified into a purely diagonal form without compromising performance (S4D; Gu et al., 2022a). By contrast, the original S4 model introduced an additional low-rank component to the diagonal structure (referred to as the Diagonal Plus Low Rank form, or DPLR) to ensure a mathematically well-founded state matrix. Notably, the diagonal variant exhibited a qualitatively similar primacy effect to the DPLR model. Due to the page limitations, results for the diagonal model are omitted from this paper, and all reported findings are based on the DPLR model.

⁷For the same reason, the proposed experimental paradigm was also inadequate for testing extended architectures of the SSM (Mamba; Gu and Dao, 2024; Dao and Gu, 2024) and the LSTM (xLSTM; Beck et al., 2024), both of which attained perfect accuracy at the highest task difficulty settings.

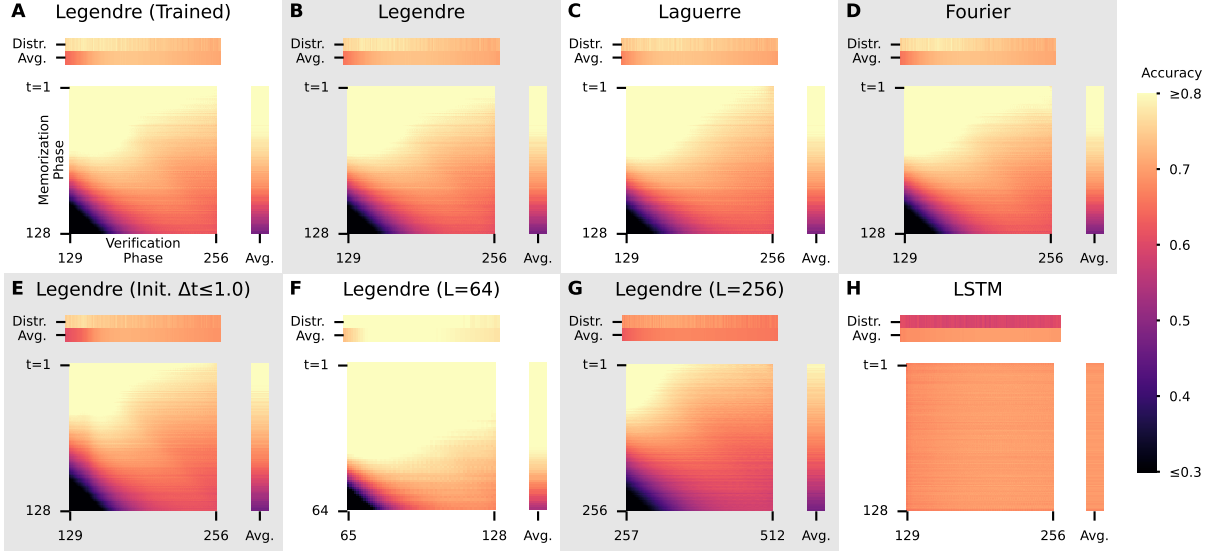


Figure 3: Accuracy of the binary memory verification task. Each cell in the square heatmaps represents the accuracy (or the recall score) for study items that were presented at the time indexed by the corresponding row and queried at the time indexed by the corresponding column. The accuracy for distractor queries is displayed in the top separate row of each panel, alongside the average accuracy across memorization times (rows). Similarly, the rightmost separate column represents the average accuracy across verification times (columns). The bottom-right panel (H) depicts the accuracy distribution for the LSTM, while the other panels (A–G) report results for the SSM (S4) model under different parameter configurations. The state and input matrices of the SSM were initialized to approximate the latent dynamics of input sequences using Legendre polynomials, except in panels C and D, where Laguerre and Fourier bases were used, respectively. The state and input matrices were optimized for the task in panel A, whereas they remained fixed at their initial values in all other panels. The discretization step size Δt was initialized in the range $0.001 \leq \Delta t \leq 0.1$, except in panel E, where the upper bound was extended to 1.0 (i.e., $0.001 \leq \Delta t \leq 1.0$). The number of study items was set to $L = 128$, except in panel F ($L = 64$) and panel G ($L = 256$).

These findings held true regardless of whether the state and input matrices of the SSM were optimized for the task (Fig. 3A) or remained fixed at their initial values (Fig. 3B–G). Moreover, the results remained consistent across different polynomial bases underlying the state and input matrices, including Laguerre (Fig. 3C), Fourier (3D), and Legendre (all other panels).

4.2 Distribution of the Time-Step Sizes

As discussed in the Preliminaries, the discretization time-step size Δt plays a critical role in determining the memory capacity of the SSM. Moreover, once the state matrix A is fixed, Δt becomes the sole parameter capable of influencing the *dynamics* of the SSM;⁸ all remaining parameters are confined to *feedforward* transforms.

Accordingly, to further investigate its role, the optimization trajectories of Δt were tracked over the course of training. The analysis revealed that as training progressed, a specific range of step sizes ($\Delta t \leq 0.03$) became dominant, compensating for the deallocation of the higher range approximately between 0.03 and 0.2 (Fig. 4).

Additionally, the peak value of Δt was found to depend on the number of the study items L ; longer study sequences led the model to favor smaller Δt values (compare the leftmost panel with the two rightmost panels).

⁸Freezing Δt resulted in a complete failure of learning.

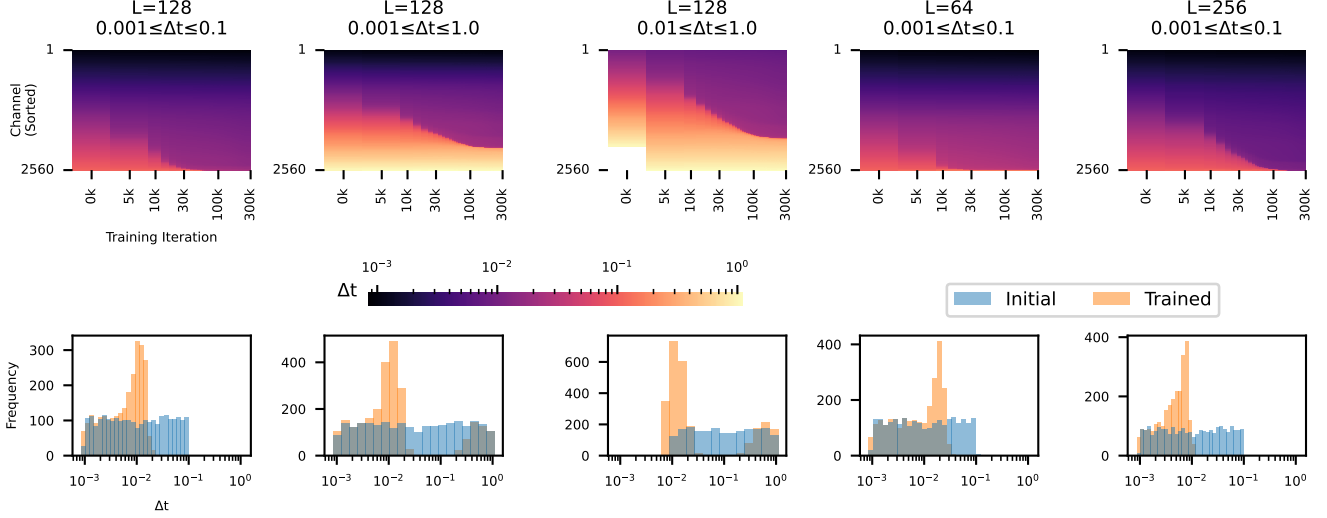


Figure 4: Top row: Optimization trajectories of the discretization step size Δt in the SSM (S4) model with frozen Legendre state and input matrices. Each heatmap column represents the distribution of Δt across 256 latent channels \times 10 training runs, sorted in the ascending order. Bottom row: Histograms displaying the initial (blue) and final (orange) values of Δt , aggregated across the 256 latent channels \times 10 training runs (see Fig. 5 in the Appendix for variations among individual runs). The first to third panel columns from the left show the results for three different ranges of log-uniformly random initializations, whereas the fourth and fifth columns tested shorter and longer study items, respectively.

5 Discussions

5.1 Summary of the Findings

The present study demonstrated that the SSM exhibits the primacy effect in memorization. When performing the binary memory verification task, which parallels paradigms used to investigate memory capacity in humans and animals (Wickelgren and Norman, 1966; Thompson and Herman, 1977; Sands and Wright, 1980; Wright et al., 1985), the model showed the highest accuracy for study items presented at the beginning of the sequence. Moreover, memorized information was not retrievable immediately after the presentation of the study items. These findings are novel and counterintuitive, as they challenge the theoretical formulation of the SSM, which assumes an exponentially decaying measure (for Legendre and Laguerre bases; Fig 1; Gu et al., 2023).

As noted in the Preliminaries, the SSM was designed to achieve a longer-lasting memory than classical RNNs (Gu et al., 2020). Prior research on RNNs and SSMs has focused on their ability to preserve input data against temporal decay. A typical benchmark for these inquiries is the delayed reconstruction task (a.k.a. the *copying memory task*; Arjovsky et al., 2016). In this task, models are provided with a *short* sequence of integers—usually ten repeatable random samples ranging between 0 and 7—followed by null inputs (e.g., zero vectors), and are then asked to reconstruct the initially observed sequence in the original order. Model performance is evaluated based on the length of the null-valued interval between the initial observations and their reconstructions.

However, little attention has been given to how the model handles longer study sequences and larger vocabularies when memory capacity reaches its limit.⁹ In particular, the question of whether the models prioritize initial/middle/recent observations has remained unexplored. The present study addressed this question and discovered that the SSM predominantly preserved the initial observations.

The key factor responsible for the primacy effect in the SSM appears to be the time-step size, Δt , as all the other trainable parameters pertain exclusively to feedforward transforms. After training on the memorization task, Δt values concentrated below a specific threshold ($\Delta t \leq 0.03$). As discussed in the Preliminaries, smaller Δt values

⁹It should be noted that the performance of the SSM can be enhanced by increasing the number of layers and/or latent channels. In this study, the model’s capacity was intentionally constrained in order to study its behavior under conditions where perfect accuracy is unattainable.

allow the model to retain more distant memories, while larger Δt values enhance the discrimination of adjacent tokens (Gu et al., 2021; Gu and Dao, 2024). The learning results thus align with the *necessary* condition for the primacy effect; however, the question remains as to why recent observations were remembered less accurately despite the exponentially decaying measure underlying the polynomial-approximation theory.

The SSMs analyzed in this study were trained from scratch on a synthetic memorization task that was designed to closely resemble controlled psychological experiments (Wickelgren and Norman, 1966; Thompson and Herman, 1977; Sands and Wright, 1980; Wright et al., 1985). Consequently, the observed primacy effect is attributed to the intrinsic properties of the SSM per se, rather than to biases introduced by data or task design. From this perspective, the present study stands in contrast to prior investigations of LLMs (Wang et al., 2023; Eicher and Irgolić, 2024; Guo and Vosoughi, 2024; Janik, 2024; Liu et al., 2024; Xiao et al., 2024); LLMs are trained on human-generated linguistic data and therefore likely to inherit the primacy effect as a byproduct of human cognitive biases embedded in the data.

5.2 Implications for Computational Neuroscience

Most existing theories of the primacy effect in human and animal memory have focused on abstract, procedural explanations of the cognitive bias. One influential account is the dual-store hypothesis (Waugh and Norman, 1965; Glanzer and Cunitz, 1966; Atkinson and Shiffrin, 1968), which attributes the primacy and recency effects to two distinct memory systems. According to this view, study items presented early in a sequence are transferred from short-term memory—where all incoming observations are temporally buffered—into long-term memory, where they are preserved against decay, thereby producing the primacy effect. By contrast, the recency effect is thought to arise from the residual information retained in short-term memory, which has limited capacity and only holds the most recent inputs.

Moving beyond such abstract accounts, several researchers have proposed biologically grounded neural network models that replicate the primacy effect (Burgess et al., 1991; Wong et al., 1991; Greene et al., 2000; Sikström, 2006; Lansner et al., 2013). The present findings align with this line of work but offer a novel perspective. Specifically, the SSM examined here was developed with the aim of advancing practically useful artificial intelligence, independently of any deliberate attempt to model the primacy effect from a psychological/biological standpoint. Thus, the spontaneous emergence of the primacy effect in the SSM presents a unique and complementary hypothesis for the mechanism underlying this cognitive bias, opening new avenues for future investigation in computational neuroscience.

Importantly, the industrial orientation of the SSM does not imply biological implausibility. Voelker and Eliasmith (2018) and Voelker et al. (2019) established a connection between the SSM and spiking neural networks, demonstrating that the dynamics of the state vector in the SSM (Eq. 1) can be implemented using a population of spiking neurons, which remain the most plausible model of biological neuronal activity to date. Moreover, Voelker and Eliasmith (2018) showed that the spiking instantiation of the SSM, when tuned to implement some particular function known as the *delay line*, reproduces the characteristic behavior of biological *time cells*,¹⁰ which have been observed in several brain regions, including the hippocampus (MacDonald et al., 2011; Eichenbaum, 2014), striatum (Mello et al., 2015), and cortex (Luczak et al., 2015). Comparing a spiking implementation of the SSM exhibiting the primacy effect with brain recordings from psychological experiments may thus yield novel insights into the neuro-computational mechanisms underlying this cognitive phenomenon.

Of course, the present study has certain limitations as a biological simulation. Most notably, the model here was explicitly optimized for the memorization task from scratch, whereas the primacy effect observed in humans and animals is presumably an outcome of their natural cognitive development. Thus, fundamentally different mechanisms may underlie the similar memorization biases exhibited by the SSM and biological organisms. Future studies may address this discrepancy by training the model in a more biologically naturalistic setting. However, as discussed in the previous section, training an ANN on empirical data, such as natural language, introduces the risk of conflating human-originated cognitive biases—transferred through the data—with the model’s intrinsic properties.

It is also important to note that the SSM does not constitute a comprehensive model of sequence memorization; its lack of the recency effect suggests the necessity of incorporating an additional module to account for short-term memory processes. Accordingly, future work should investigate whether the SSM can reliably function as a long-term memory component when integrated with a complementary short-term memory mechanism (e.g., finite-queue/Markov systems), either through modular combination or ensemble learning.

¹⁰Time cells fire at specific moments following onset cues/events and are believed to encode temporal information (MacDonald et al., 2011).

The model’s capacity also far exceeded that of biological memory systems. The binary memory verification task employed in this study involved extremely long lists of study items ($L \in \{64, 128, 256\}$) as well as a huge vocabulary ($K = 4096$), which is unlikely to be replicated in human or animal experiments. This level of task difficulty was necessary to clearly demonstrate the primacy effect in the SSM, and was still insufficient to reach the memory limits of more powerful architectures such as Mamba (Gu and Dao, 2024; Dao and Gu, 2024) and xLSTM (Beck et al., 2024), thereby constraining the scope of model comparison here. Future research should explore downscaling the model toward more biologically plausible conditions.

Finally, the present study does not offer an explanation for various well-documented characteristics of the psychological primacy effect. For instance, the retention of initial study items is thought to be achieved, or at least facilitated, by *rehearsal*—repetitive mental or verbal recitation of observed items before requested recall/verification (Rundus, 1971; Marshall and Werder, 1972; Glenberg et al., 1980)—for which the models studied here lack an analogous mechanism.

In addition, the models operated on a unitless discrete time scale, to which the continuous-time representation of the SSM was aligned. As a result, they are unsuitable for investigating physical-time effects, such as the impact of retention intervals between study-item presentation and verification (Cornell and Bergstrom, 1983; Wright et al., 1985; Neath, 1993) or variations in inter-item intervals (Neath and Knodler, 1994). This limitation could be addressed by exploring spiking neural networks equivalent the SSM. As noted above, the SSM can be converted into a spiking neural network, which in turn enables the simulation of the physical-time effects as well as the incorporation of biologically inspired connectivity structures (Voelker and Eliasmith, 2018).

Acknowledgments

This study was supported by JST ACT-X (JPMJAX21AN) and Core Research for Evolutional Science and Technology (JPMJCR22P5); JSPS Grant-in-Aid for Early-Career Scientists (JP21K17805) and for Scientific Research A (JP24H00774), B (JP22H03914), and C (JP24K15087); and Kayamori Foundation of Informational Science Advancement (K35XXVIII620). The author also gratefully acknowledges the support of the ACCMS, Kyoto University, regarding the use of their supercomputer system.

References

- Arjovsky, M., Shah, A., and Bengio, Y. (2016). Unitary evolution recurrent neural networks. In Balcan, M. F. and Weinberger, K. Q., editors, *Proceedings of The 33rd International Conference on Machine Learning*, volume 48 of *Proceedings of Machine Learning Research*, pages 1120–1128, New York, New York, USA. PMLR.
- Atkinson, R. C. and Shiffrin, R. M. (1968). Human memory: A proposed system and its control processes. In Spence, K. W. and Spence, J. T., editors, *Psychology of Learning and Motivation*, volume 2 of *Psychology of Learning and Motivation*, pages 89–195. Academic Press.
- Beck, M., Pöppel, K., Spanring, M., Auer, A., Prudnikova, O., Kopp, M., Klambauer, G., Brandstetter, J., and Hochreiter, S. (2024). xLSTM: Extended long short-term memory. In Globerson, A., Mackey, L., Belgrave, D., Fan, A., Paquet, U., Tomczak, J., and Zhang, C., editors, *Advances in Neural Information Processing Systems*, volume 37, pages 107547–107603. Curran Associates, Inc.
- Bengio, Y., Simard, P., and Frasconi, P. (1994). Learning long-term dependencies with gradient descent is difficult. *IEEE Transactions on Neural Networks*, 5(2):157–166.
- Burgess, N., Shapiro, J. L., and Moore, M. A. (1991). Neural network models of list learning. *Network: Computation in Neural Systems*, 2(4):399.
- Chang, S., Zhang, Y., Han, W., Yu, M., Guo, X., Tan, W., Cui, X., Witbrock, M., Hasegawa-Johnson, M. A., and Huang, T. S. (2017). Dilated recurrent neural networks. In Guyon, I., Luxburg, U. V., Bengio, S., Wallach, H., Fergus, R., Vishwanathan, S., and Garnett, R., editors, *Advances in Neural Information Processing Systems*, volume 30. Curran Associates, Inc.
- Chen, Y., Gilroy, S., Maletti, A., May, J., and Knight, K. (2018). Recurrent neural networks as weighted language recognizers. In Walker, M., Ji, H., and Stent, A., editors, *Proceedings of the 2018 Conference of the North American Chapter of the Association for Computational Linguistics: Human Language Technologies, Volume 1 (Long Papers)*, pages 2261–2271, New Orleans, Louisiana. Association for Computational Linguistics.
- Cornell, E. H. and Bergstrom, L. I. (1983). Serial-position effects in infants’ recognition memory. *Memory & Cognition*, 11(5):494–499.
- Cuturi, M. (2013). Sinkhorn distances: Lightspeed computation of optimal transport. In Burges, C., Bottou, L., Welling, M., Ghahramani, Z., and Weinberger, K., editors, *Advances in Neural Information Processing Systems*, volume 26. Curran Associates, Inc.
- Dao, T. and Gu, A. (2024). Transformers are SSMS: Generalized models and efficient algorithms through structured state space duality. In Salakhutdinov, R., Koltner, Z., Heller, K., Weller, A., Oliver, N., Scarlett, J., and Berkenkamp, F., editors, *Proceedings of the 41st International Conference on Machine Learning*, volume 235 of *Proceedings of Machine Learning Research*, pages 10041–10071. PMLR.
- Ebbinghaus, H. (1913). *Memory: A contribution to experimental psychology*. Teachers College Press.
- Eichenbaum, H. (2014). Time cells in the hippocampus: a new dimension for mapping memories. *Nature Reviews Neuroscience*, 15(11):732–744.
- Eicher, J. E. and Irgolić, R. F. (2024). Reducing selection bias in large language models.
- Elman, J. L. (1990). Finding structure in time. *Cognitive Science*, 14(2):179–211.
- Glanzer, M. and Cunitz, A. R. (1966). Two storage mechanisms in free recall. *Journal of Verbal Learning and Verbal Behavior*, 5(4):351–360.
- Glenberg, A. M., Bradley, M. M., Stevenson, J. A., Kraus, T. A., Tkachuk, M. J., Gretz, A. L., Fish, J. H., and Turpin, B. M. (1980). A two-process account of long-term serial position effects. *Journal of Experimental Psychology: Human Learning and Memory*, 6(4):355–369.
- Graves, A. (2013). Generating sequences with recurrent neural networks. arXiv:1308.0850.

- Greene, A. J., Prepscius, C., and Levy, W. B. (2000). Primacy versus recency in a quantitative model: Activity is the critical distinction. *Learning & Memory*, 7(1):48–57.
- Gu, A. and Dao, T. (2024). Mamba: Linear-time sequence modeling with selective state spaces. In *Proceedings of the First Conference on Language Modeling*.
- Gu, A., Dao, T., Ermon, S., Rudra, A., and Ré, C. (2020). HiPPO: Recurrent memory with optimal polynomial projections. In Larochelle, H., Ranzato, M., Hadsell, R., Balcan, M., and Lin, H., editors, *Advances in Neural Information Processing Systems*, volume 33, pages 1474–1487. Curran Associates, Inc.
- Gu, A., Goel, K., Gupta, A., and Ré, C. (2022a). On the parameterization and initialization of diagonal state space models. In Koyejo, S., Mohamed, S., Agarwal, A., Belgrave, D., Cho, K., and Oh, A., editors, *Advances in Neural Information Processing Systems*, volume 35, pages 35971–35983. Curran Associates, Inc.
- Gu, A., Goel, K., and Ré, C. (2022b). Efficiently modeling long sequences with structured state spaces. In *Proceedings of the Tenth International Conference on Learning Representations (ICLR)*. OpenReview.net.
- Gu, A., Johnson, I., Goel, K., Saab, K., Dao, T., Rudra, A., and Ré, C. (2021). Combining recurrent, convolutional, and continuous-time models with linear state space layers. In Ranzato, M., Beygelzimer, A., Dauphin, Y., Liang, P., and Vaughan, J. W., editors, *Advances in Neural Information Processing Systems*, volume 34, pages 572–585. Curran Associates, Inc.
- Gu, A., Johnson, I., Timalsina, A., Rudra, A., and Ré, C. (2023). How to train your HIPPO: State space models with generalized orthogonal basis projections. In *Proceedings of the Eleventh International Conference on Learning Representations (ICLR)*. OpenReview.net.
- Guo, X. and Vosoughi, S. (2024). Serial position effects of large language models.
- He, K., Zhang, X., Ren, S., and Sun, J. (2016). Deep residual learning for image recognition. In *The IEEE Conference on Computer Vision and Pattern Recognition (CVPR)*, pages 770–778.
- Hochreiter, S. and Schmidhuber, J. (1997). Long short-term memory. *Neural Computation*, 9(8):1735–1780.
- Jaeger, H. (2001). Short term memory in echo state networks. Technical report, German National Research Center for Information Technology, Sankt Augustin.
- Jaeger, H. and Haas, H. (2004). Harnessing nonlinearity: Predicting chaotic systems and saving energy in wireless communication. *Science*, 304(5667):78–80.
- Janik, R. A. (2024). Aspects of human memory and large language models.
- Jing, L., Gulcehre, C., Peurifoy, J., Shen, Y., Tegmark, M., Soljacic, M., and Bengio, Y. (2019). Gated orthogonal recurrent units: On learning to forget. *Neural Computation*, 31(4):765–783.
- Jing, L., Shen, Y., Dubcek, T., Peurifoy, J., Skirlo, S., LeCun, Y., Tegmark, M., and Soljačić, M. (2017). Tunable efficient unitary neural networks (EUNN) and their application to RNNs. In Precup, D. and Teh, Y. W., editors, *Proceedings of the 34th International Conference on Machine Learning*, volume 70 of *Proceedings of Machine Learning Research*, pages 1733–1741. PMLR.
- Kalchbrenner, N., Elsen, E., Simonyan, K., Noury, S., Casagrande, N., Lockhart, E., Stimberg, F., van den Oord, A., Dieleman, S., and Kavukcuoglu, K. (2018). Efficient neural audio synthesis. In Dy, J. and Krause, A., editors, *Proceedings of the 35th International Conference on Machine Learning*, volume 80 of *Proceedings of Machine Learning Research*, pages 2410–2419. PMLR.
- Kingma, D. P. and Ba, J. (2015). Adam: A method for stochastic optimization. In *Proceedings of 3rd International Conference on Learning Representations (ICLR)*, San Diego, California.
- Lansner, A., Marklund, P., Sikström, S., and Nilsson, L.-G. (2013). Reactivation in working memory: An attractor network model of free recall. *PLOS ONE*, 8(8):1–11.

- Liu, N. F., Lin, K., Hewitt, J., Paranjape, A., Bevilacqua, M., Petroni, F., and Liang, P. (2024). Lost in the middle: How language models use long contexts. *Transactions of the Association for Computational Linguistics*, 12:157–173.
- Loshchilov, I. and Hutter, F. (2017). SGDR: stochastic gradient descent with warm restarts. In *Proceedings of the 5th International Conference on Learning Representations (ICLR)*. OpenReview.net.
- Luczak, A., McNaughton, B. L., and Harris, K. D. (2015). Packet-based communication in the cortex. *Nature Reviews Neuroscience*, 16(12):745–755.
- MacDonald, C. J., Lepage, K. Q., Eden, U. T., and Eichenbaum, H. (2011). Hippocampal “time cells” bridge the gap in memory for discontinuous events. *Neuron*, 71(4):737–749.
- Marshall, P. H. and Werder, P. R. (1972). The effects of the elimination of rehearsal on primacy and recency. *Journal of Verbal Learning and Verbal Behavior*, 11(5):649–653.
- Mello, G. B., Soares, S., and Paton, J. J. (2015). A scalable population code for time in the striatum. *Current Biology*, 25(9):1113–1122.
- Miller, G. A. (1956). The magical number seven, plus or minus two: Some limits on our capacity for processing information. *Psychological Review*, 63(2):81–97.
- Murdock, B. B. (1962). The serial position effect of free recall. *Journal of Experimental Psychology*, 64(5):482–488.
- Neath, I. (1993). Distinctiveness and serial position effects in recognition. *Memory & Cognition*, 21(5):689–698.
- Neath, I. and Knodler, A. J. (1994). Distinctiveness and serial position effects in recognition and sentence processing. *Journal of Memory and Language*, 33(6):776–795.
- Neil, D., Pfeiffer, M., and Liu, S.-C. (2016). Phased lstm: Accelerating recurrent network training for long or event-based sequences. In Lee, D., Sugiyama, M., Luxburg, U., Guyon, I., and Garnett, R., editors, *Advances in Neural Information Processing Systems*, volume 29. Curran Associates, Inc.
- Rundus, D. (1971). Analysis of rehearsal processes in free recall. *Journal of Experimental Psychology*, 89(1):63–77.
- Sands, S. F. and Wright, A. A. (1980). Primate memory: Retention of serial list items by a rhesus monkey. *Science*, 209(4459):938–940.
- Shi, X., Chen, Z., Wang, H., Yeung, D.-Y., Wong, W.-k., and WOO, W.-c. (2015). Convolutional LSTM network: A machine learning approach for precipitation nowcasting. In Cortes, C., Lawrence, N., Lee, D., Sugiyama, M., and Garnett, R., editors, *Advances in Neural Information Processing Systems*, volume 28. Curran Associates, Inc.
- Siegelmann, H. T. (1999). *Neural Networks and Analog Computation: Beyond the Turing Limit*. Birkhauser Boston Inc., Cambridge, MA, USA.
- Siegelmann, H. T. and Sontag, E. D. (1992). On the computational power of neural nets. In *Proceedings of the Fifth Annual Workshop on Computational Learning Theory, COLT ’92*, pages 440–449, New York, NY, USA. Association for Computing Machinery.
- Siegelmann, H. T. and Sontag, E. D. (1995). On the computational power of neural nets. *Journal of Computer and System Sciences*, 50(1):132–150.
- Sikström, S. (2006). The isolation, primacy, and recency effects predicted by an adaptive LTD/LTP threshold in postsynaptic cells. *Cognitive Science*, 30(2):243–275.
- Sundermeyer, M., Schlüter, R., and Ney, H. (2012). LSTM neural networks for language modeling. In *Proceedings of INTERSPEECH*, pages 194–197.
- Thompson, R. K. R. and Herman, L. M. (1977). Memory for lists of sounds by the bottle-nosed dolphin: Convergence of memory processes with humans? *Science*, 195(4277):501–503.

- Tustin, A. (1947). A method of analysing the behaviour of linear systems in terms of time series. *Journal of the Institution of Electrical Engineers - Part IIA: Automatic Regulators and Servo Mechanisms*, 94:130–142.
- Vaswani, A., Shazeer, N., Parmar, N., Uszkoreit, J., Jones, L., Gomez, A. N., Kaiser, L. u., and Polosukhin, I. (2017). Attention is all you need. In Guyon, I., Luxburg, U. V., Bengio, S., Wallach, H., Fergus, R., Vishwanathan, S., and Garnett, R., editors, *Advances in Neural Information Processing Systems 30*, pages 5998–6008. Curran Associates, Inc.
- Voelker, A., Kajić, I., and Eliasmith, C. (2019). Legendre memory units: Continuous-time representation in recurrent neural networks. In Wallach, H., Larochelle, H., Beygelzimer, A., d'Alché-Buc, F., Fox, E., and Garnett, R., editors, *Advances in Neural Information Processing Systems*, volume 32. Curran Associates, Inc.
- Voelker, A. R. and Eliasmith, C. (2018). Improving spiking dynamical networks: Accurate delays, higher-order synapses, and time cells. *Neural Computation*, 30(3):569–609.
- Wang, Y., Cai, Y., Chen, M., Liang, Y., and Hooi, B. (2023). Primacy effect of ChatGPT. In Bouamor, H., Pino, J., and Bali, K., editors, *Proceedings of the 2023 Conference on Empirical Methods in Natural Language Processing*, pages 108–115, Singapore. Association for Computational Linguistics.
- Waugh, N. C. and Norman, D. A. (1965). Primary memory. *Psychological Review*, 72(2):89–104.
- Weiss, G., Goldberg, Y., and Yahav, E. (2018). On the practical computational power of finite precision rnns for language recognition. In *Proceedings of the 56th Annual Meeting of the Association for Computational Linguistics (Volume 2: Short Papers)*, pages 740–745. Association for Computational Linguistics.
- Wickelgren, W. A. and Norman, D. A. (1966). Strength models and serial position in short-term recognition memory. *Journal of Mathematical Psychology*, 3(2):316–347.
- Wong, K. Y. M., Kahn, P. E., and Sherrington, D. (1991). A neural network model of working memory exhibiting primacy and recency. *Journal of Physics A: Mathematical and General*, 24(5):1119.
- Wright, A. A., Santiago, H. C., Sands, S. F., Kendrick, D. F., and Cook, R. G. (1985). Memory processing of serial lists by pigeons, monkeys, and people. *Science*, 229(4710):287–289.
- Xiao, G., Tian, Y., Chen, B., Han, S., and Lewis, M. (2024). Efficient streaming language models with attention sinks. In *Proceedings of the Twelfth International Conference on Learning Representations (ICLR)*. OpenReview.net.
- Zhang, J., Lin, Y., Song, Z., and Dhillon, I. (2018). Learning long term dependencies via Fourier recurrent units. In Dy, J. and Krause, A., editors, *Proceedings of the 35th International Conference on Machine Learning*, volume 80 of *Proceedings of Machine Learning Research*, pages 5815–5823. PMLR.

A Appendix

A.1 Remarks on Transformer

As noted in the Methods section, the present study was unable to assess whether or not Transformer exhibits the primacy effect (without inheriting human-induced biases). Specifically, the model consistently achieved perfect accuracy on the binary memory verification task, thereby failing to encounter the memory load necessary for evaluating the primacy effect. This section offers a theoretical account of how Transformer is able to solve this task, with particular focus on the role of its attention mechanism.

to begin, recall that the “memory” in Transformer (and other finite-queue/Markov models in general) consists of the *raw* input observation, preserved without decay or lossy compression. Although this approach is highly non-economic for processing long sequences, growing computational resources have made it viable in practice.

Given full access to the uncompressed sequence of prior observations, Transformer computes attention weights based on the dot-product similarity between (linear projected) input embeddings. In the context of the memory verification task, this computation enables a direct comparison between the study items and verification queries; setting aside the interference from positional encodings, the resulting attention distribution at each verification time step becomes sharply peaked (one-hot-like) when the query matches a study item, or almost uniform when it does not. As a result, Transformer can trivially solve the task by exploiting this attention distribution.

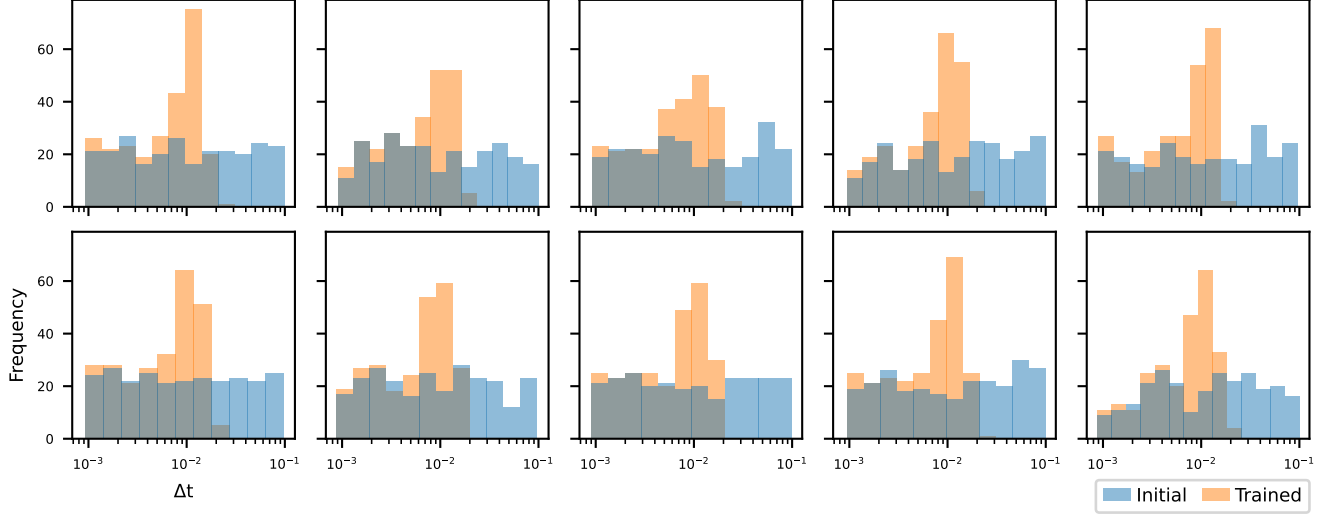


Figure 5: Histograms displaying the initial (blue) and final (orange) values of Δt . Each panel presents the distributions obtained from one of the ten training runs with different random seeds.

A.2 Distributions of Δt across Training Runs

Fig. 5 reports the distribution of the Δt parameters before and after each of the ten training runs (decomposing the leftmost panel in Fig. 4).